

Langerhans Cells Facilitate UVB-Induced Epidermal Carcinogenesis

Julia M. Lewis¹, Christina D. Bürgler¹, Marianna Freudzon¹, Kseniya Golubets¹, Juliet F. Gibson¹, Renata B. Filler¹ and Michael Girardi¹

UVB light is considered the major environmental inducer of human keratinocyte (KC) DNA mutations, including within the tumor-suppressor gene p53, and chronic exposure is associated with cutaneous squamous cell carcinoma formation. Langerhans cells (LCs) comprise a dendritic network within the suprabasilar epidermis, yet the role of LCs in UVB-induced carcinogenesis is largely unknown. Herein we show that LC-intact epidermis develops UVB-induced tumors more readily than LC-deficient epidermis. Although levels of epidermal cyclopuridine dimers following acute UVB exposure are equivalent in the presence or absence of LCs, chronic UVB-induced p53 mutant clonal islands expand more readily in association with LCs, which remain largely intact and are preferentially found in proximity to the expanding mutant KC populations. The observed LC facilitation of mutant p53 clonal expansion is completely $\alpha\beta$ and $\gamma\delta$ T-cell independent and is associated with increased intraepidermal expression of IL-22 and the presence of group 3 innate lymphoid cells. These data demonstrate that LCs have a key role in UVB-induced cutaneous carcinogenesis and suggest that LCs locally stimulate KC proliferation and innate immune cells that provoke tumor outgrowth.

Journal of Investigative Dermatology (2015) **135**, 2824–2833; doi:10.1038/jid.2015.207; published online 25 June 2015

INTRODUCTION

Chronic UVB light exposure is a major risk factor for development of premalignant actinic keratoses and malignant squamous cell carcinoma (SCC), each harboring frequent mutations in the master cell cycle regulator TP53 (p53) gene (Ziegler *et al.*, 1994). Initiating mutations largely result from unrepaired cyclopuridine dimers (CPDs). Promoting oncogenetic alterations, e.g., RAS (Daya-Grosjean *et al.*, 1993) and NOTCH (Durinck *et al.*, 2011), may result from continued UV exposure, immune influences, and other stimuli that drive keratinocyte (KC) proliferation, dedifferentiation, transformation, and ultimately tumor outgrowth (reviewed in Epstein, 1983; Kripke, 1984). Situated adjacent to basal and folliculo-infundibular KCs that give rise to actinic keratoses and SCC neoplasia is a network of dendritic CD207+ (Langerin+) intraepidermal Langerhans cells (LCs) that (1) survey the epidermis (Nishibu *et al.*, 2006) for

evidence of toxin/microbial penetration (Kubo *et al.*, 2009) and (2) serve as antigen-presenting cells for the activation of T cells resident in the skin (Seneschal *et al.*, 2012) or after migration to draining lymph nodes (Kaplan *et al.*, 2005; Bobr *et al.*, 2012).

We have previously suggested that LCs may function as key players in the epithelial stress response, where they coordinate with resident $\gamma\delta$ T cells and $\alpha\beta$ natural killer (NK) T cells (Strid *et al.*, 2008). $\gamma\delta$ T cells (Girardi *et al.*, 2001, 2003), including resident $\gamma\delta$ dendritic epidermal T cells (DETCs) (Strid *et al.*, 2008; MacLeod *et al.*, 2014), may mediate diverse antitumor activities, while LCs have been shown to facilitate chemical carcinogenesis by enhancing mutagenesis (Modi *et al.*, 2012) and tumor promotion (Lewis *et al.*, 2014). Moreover, the role of LC in the well-established phenomenon of UV-induced immune suppression is unclear, with some evidence suggesting that LC are not necessary (Wang *et al.*, 2009) and other studies suggesting that LCs may have a critical role (Fukunaga *et al.*, 2010). Hence, we sought to determine whether locally resident LC influence events relevant to UV induction of cutaneous SCC, and if so, whether such influences are dependent on adaptive and innate immunity afforded by $\alpha\beta$ and/or $\gamma\delta$ T cells. We utilized mice rendered genetically deficient in LCs (Kaplan *et al.*, 2005), and/or $\alpha\beta$ and $\gamma\delta$ T cells, and studied the impact on several fundamental steps of UVB-induced cutaneous carcinogenesis, including direct genotoxicity (CPD formation), p53 mutant clonal KC development and expansion, and tumor outgrowth. Herein, we reveal that LC exert T-cell-independent pro-tumor effects largely via the promotion of clonal

¹Department of Dermatology, Yale School of Medicine, New Haven, Connecticut, USA

Correspondence: Michael Girardi, Department of Dermatology, Yale University School of Medicine, 333 Cedar Street, HRT 604D, New Haven, Connecticut 06520-8059, USA. E-mail: girardi@yale.edu

Sites of experiments: New Haven, Connecticut, USA.

Abbreviations: CPD, cyclopuridine dimer; DC, dendritic cell; DETC, dendritic epidermal T cell; DTA, LC-deficient hu-Langerin-DTA transgenic; ILC, innate lymphoid cell; KC, keratinocyte; LC, Langerhans cell; NK, natural killer; NLC, normal littermate control; SCC, squamous cell carcinoma; TPA, 12-O-tetradecanoylphorbol-13-acetate

Received 12 January 2015; revised 21 May 2015; accepted 25 May 2015; accepted article preview online 8 June 2015; published online 25 June 2015

expansion in association with enhanced epidermal expression of IL-1 β , IL-6, IL-23, and nitric oxide synthase 2, inducible (NOS2), as well as augmented expression of the epithelial growth factor IL-22. In addition, we observe group 3 innate lymphoid cells (ILC3) capable of IL-22 production in chronically UVB irradiated epidermis. Furthermore, we identify a major T-cell-independent role for LCs in the regulation of the epidermal stress response more generally.

RESULTS

LCs enhance chronic UVB-induced cutaneous tumor outgrowth

To assess the collective effect of chronic UVB exposure on the emergence of cutaneous tumors, hairless (hr/hr) LC-deficient hu-Langerin-DTA transgenic (DTA) mice (Kaplan *et al.*, 2005) were compared with LC-intact normal littermate controls (NLC) for tumor induction by 3 \times weekly UVB irradiation of dorsal skin. LC-intact mice showed a substantially higher rate of UVB-induced tumor development (mean 5.10 ± 1.18 vs. 2.44 ± 0.47 tumors/mouse at 18 weeks; $P=0.002$) (Figure 1a), as well as a greater accumulating tumor volume over this time (Figure 1b). UVB exposure has been shown to compromise intraepidermal LC numbers via induction of apoptosis and stimulation of LC migration (Aberer *et al.*, 1986; Nishibu *et al.*, 2006). Thus we considered the possibility that the observed pro-tumor influence of LC might be due to early events, e.g., specifically by facilitating KC DNA damage.

LCs do not affect UVB-induced CPDs in neighboring KCs

In chemical carcinogenesis, LCs are associated with dimethylbenz[a]anthracene-induced genotoxicity in adjacent KCs (Modi *et al.*, 2012). As LCs are also associated with accelerated UVB-induced tumor development, we considered the possibility that CPD formation might occur more readily in the presence of LCs. Given that $\gamma\delta$ DETCs have shown the capacity to facilitate CPD repair (MacLeod *et al.*, 2014) and LC and $\gamma\delta$ DETCs form tightly regulated cell

contacts following epidermal stress (Strid *et al.*, 2008), we also considered whether LCs might effect the efficient repair of CPDs within KCs. Groups of LC-intact (NLC) and LC-deficient (DTA) mice were irradiated with a single dose of 50 or 100 J m $^{-2}$ UVB, and epidermal sheets were harvested at 1 hour to assess for acute UVB-induced CPD formation and at 24 hours to assess CPD repair (Figure 2a and b; Supplementary Figure S1 online). CPDs were observed diffusely within basal KCs 1 hour after UVB exposure, significantly higher at 100 J m $^{-2}$ than at 50 J m $^{-2}$ but indistinguishable between similarly exposed NLC and DTA mice. At 24 hours after UVB exposure, CPD level decreased comparably between NLC and DTA skin (Figure 2a and b) while LC numbers were maintained throughout (Figure 2c). These data suggest that LCs do not significantly influence CPD formation following UVB exposure, nor do they appear to affect DNA repair in the first 24 hours following exposure. Thus we focused further experiments on the effects of LCs on KCs during chronic UVB exposure.

LC numbers are largely maintained in chronically UVB-irradiated epidermis

Prior studies have demonstrated the sensitivity of LCs to acute UVB-induced apoptosis, as well as the capacity of UVB to trigger LC migration to draining lymph nodes (Aberer *et al.*, 1986; Nishibu *et al.*, 2006). UVB can also precipitate epidermotropism and differentiation of peripheral blood Gr1+ monocytes into CD207+ dendritic cells (DCs) (Merad *et al.*, 2002) followed by a second wave of steady-state precursor-derived long-term LCs (Seré *et al.*, 2012) to repopulate the LC compartment. Few studies, however, have quantified the net effects of chronic UVB exposure on the intraepidermal LC population. As it was unlikely that the increased tumor susceptibility observed in LC-intact skin (Figure 1) was due to LC enhancement of direct DNA damage in adjacent KCs (Figure 2), we hypothesized that under chronic low-dose UVB exposure net LC numbers would remain largely intact. Untreated NLC and DTA mice displayed comparable $\gamma\delta$ DETC density (Figure 3a, b and c), consistent with prior reports (Kaplan *et al.*, 2005). Following 5 weeks chronic UVB exposure, within NLC mice we found that the LC compartment was largely maintained; in contrast, intraepidermal $\gamma\delta$ T cells were nearly eliminated in both NLC and DTA, consistent with the exquisite sensitivity (Ho *et al.*, 1991) of DETCs to UVB-induced apoptosis (Figure 3a, b and c).

LCs promote p53 mutant KC clonal island expansion and are preferentially found in association with the p53 mutant islands

To address the potential role of LCs in the enhancement of clonal expansion, hairless (hr/hr) LC-intact (NLC) and LC-deficient (DTA) mice were exposed to UVB, and p53 mutant KC clonal islands were quantified at 5 and 9 weeks (e.g., 6–10 weeks prior to tumor onset). “p53 islands” can be identified in UVB-exposed epidermis by staining with an antibody that binds to both native and mutant p53 but at markedly higher levels in KCs harboring mutant p53 due to the absence of negative feedback. Direct sequencing of p53 has shown that such p53-immunopositive islands are mutant and clonal (Zhang *et al.*, 2001). To confirm active

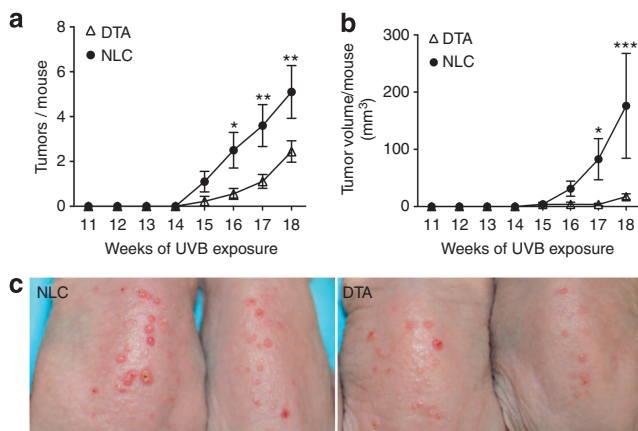


Figure 1. Langerhans cells (LCs) influence UVB-induced cutaneous tumor development. Carcinogenesis was induced in hairless (hr/hr) LC-intact (normal littermate controls (NLC)) and LC-deficient (hu-Langerin-DTA transgenic (DTA)) mice by exposure to 400 J m $^{-2}$ UVB three times per week. Increased (a) tumor number and (b) volume were seen in the presence of LC ($n=10$ NLC, 9 DTA, $*P<0.05$, $**P<0.01$, $***P<0.001$). (c) Representative images from a and b.

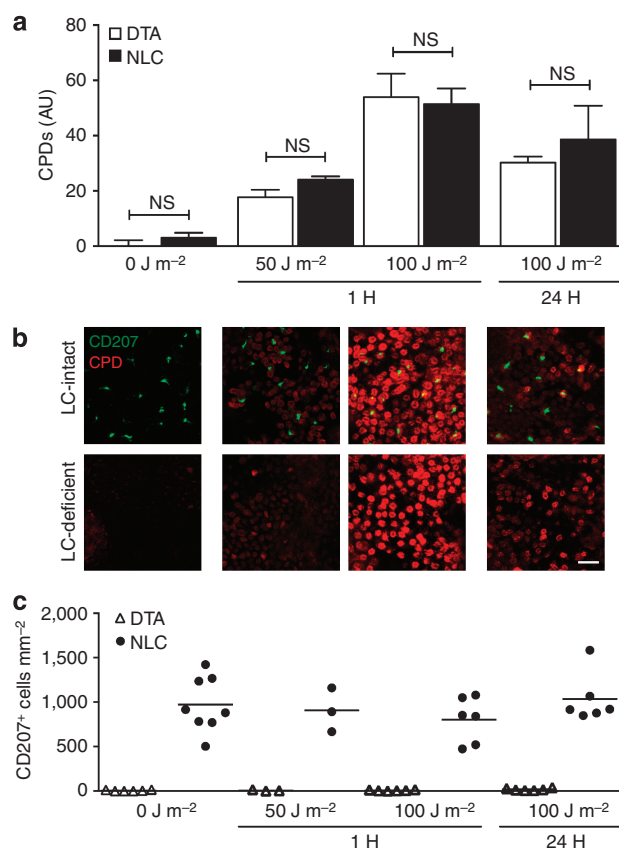


Figure 2. Langerhans cells (LCs) do not affect UVB-induced cyclopuridine dimer (CPD) formation. (a) Hairless (hr/hr) LC-intact (normal littermate controls (NLC)) and LC-deficient (LC-deficient hu-Langerin-DTA transgenic (DTA)) mice were treated with a single dose of UVB and epidermal sheets prepared 1 or 24 hours later and stained with antibodies directed against thymine dimers (CPD) and CD207 plus the nuclear dye To-Pro-3 (shown in Supplementary Figure S1 online). CPD fluorescence intensity was similar in LC-intact and LC-deficient mice. (b) Representative images from a show CPD (red) and LC (CD207, green). Scale bar=20 μ m. (c) LC density does not change during the 24 hours following a single dose of UVB. $n=3-8$ mice/group; in c, each symbol represents one mouse. NS, not significant.

proliferation of the p53 mutant KCs, we performed co-staining with Ki-67 (Supplementary Figure S2 online). Although p53 island number and basal area occupied were comparable between NLC and DTA mice at 5 weeks, NLC showed a >50% greater number of p53 islands and a >100% increase in the basal area involved at 9 weeks (Figure 3d and e; Supplementary Figure S3 online), with similar results seen when hair-bearing FVB.NLC and FVB.DTA mice were compared (Supplementary Figure S4 online).

Thus persistent and/or repopulating LCs are available in sufficient numbers under chronic UVB exposure to influence epidermal tumor outgrowth. Moreover, LCs were preferentially found within or adjacent to p53 clonal islands (Figure 3f and i, Supplementary Figure S3 online), with a ~40% increase in LC density in association with the mutant KCs after 9 weeks of chronic UVB exposure (Figure 3i, 617 ± 35 mm⁻² island associated, 448 ± 44 mm⁻² not associated, $P=0.0065$). Phenotypic analysis of LCs isolated from chronic UVB-exposed epidermis revealed upregulation of CD207 and

major histocompatibility complex II (MHC-II), consistent with LC activation, but without changes in C-C chemokine receptor 7 or C-X-C chemokine receptor 4 expression, which might have otherwise indicated an increased capacity for migration to draining lymph nodes (Supplementary Figure S5 online).

LC enhancement of p53 mutant KC clonal expansion is T-cell independent

As LCs may function as antigen-presenting cells, we next assessed the contribution of $\alpha\beta$ and $\gamma\delta$ T cells to the mechanism of LC enhancement of p53 mutant KC clonal expansion. DTA mice were intercrossed to TCR $\beta^{-/-}$ (deficient in all $\alpha\beta$ T-cell populations) and TCR $\delta^{-/-}$ (deficient in all $\gamma\delta$ T-cell populations). LC-intact but T cell-deficient (TCR $\beta^{-/-}$ $\delta^{-/-}$.NLC) mice were compared with LC-deficient and T-cell-deficient (TCR $\beta^{-/-}$ $\delta^{-/-}$.DTA) mice for the development and expansion of p53 mutant KC islands under chronic UVB exposure (Figure 4). In the complete absence $\alpha\beta$ or $\gamma\delta$ T cells, p53 island development and growth was again substantially enhanced in the presence of LCs. Following 9 weeks of UVB exposure, p53 island density was 86% increased in TCR $\beta^{-/-}$ $\delta^{-/-}$.NLC versus TCR $\beta^{-/-}$ $\delta^{-/-}$.DTA (Figure 4a, 79.9 ± 4.5 vs. 42.9 ± 4.3 cm⁻², $P<0.0001$) and p53 island area was increased by 135% (Figure 4b, 10661 ± 1188 vs. 4520 ± 711 μ m² p53 island mm⁻², $P=0.0004$). The lack of requirement for $\alpha\beta$ T cells suggests that the mechanism does not involve LC stimulation of immunosuppressive $\alpha\beta$ regulatory T cells (Shreedhar *et al.*, 1998) or NK T cells (Fukunaga *et al.*, 2010) previously implicated in UV-induced immune suppression, $\gamma\delta$ T cells with the capacity for cytotoxicity of transformed KCs (Girardi *et al.*, 2001), or pro-inflammatory $\alpha\beta$ (Kwong *et al.*, 2010) and $\gamma\delta$ (Wakita *et al.*, 2010) T-cell subsets that might drive mutant KC proliferation. The striking parallel of the dependence on LCs for increased p53 island number and size, as well as the LC association with the expanding p53 islands, observed in both T-cell-intact (Figure 3d, e and i) and T cell-deficient (Figure 4a, b and c) mice, underscores the fundamental pro-tumor contribution of LCs and suggested an underlying paracrine effect.

We thus sought to quantify within naive and chronically UVB-irradiated TCR $\beta^{-/-}$ $\delta^{-/-}$.NLC and TCR $\beta^{-/-}$ $\delta^{-/-}$.DTA epidermis the expression levels of several epithelial growth factors previously implicated in paracrine stimulation of epithelial proliferation and neoplasia (Figure 4d): epidermal growth factor (Chan *et al.*, 2004), amphiregulin (Rittié *et al.*, 2006), insulin-like growth factor-1 (DiGiovanni *et al.*, 2000), keratinocyte growth factor-1/fibroblast growth factor-7 (Jameson *et al.*, 2002; Chikama *et al.*, 2008), and IL-22 (Briso *et al.*, 2013; Rabeony *et al.*, 2014). Epidermal cells from the non-irradiated skin of TCR $\beta^{-/-}$ $\delta^{-/-}$.NLC and TCR $\beta^{-/-}$ $\delta^{-/-}$.DTA revealed expression profiles consistent with constitutive expression of IL-22 within LC-intact epidermis (mean fold change untreated DTA = 1.0 ± 0.1 vs. untreated NLC = 8.4 ± 2.1 , $P=0.0023$), with levels of such substantially elevated following chronic UVB exposure (DTA+UVB = 1.6 ± 0.1 vs. untreated DTA, $P=0.0029$; NLC+UVB = 52.5 ± 7.1

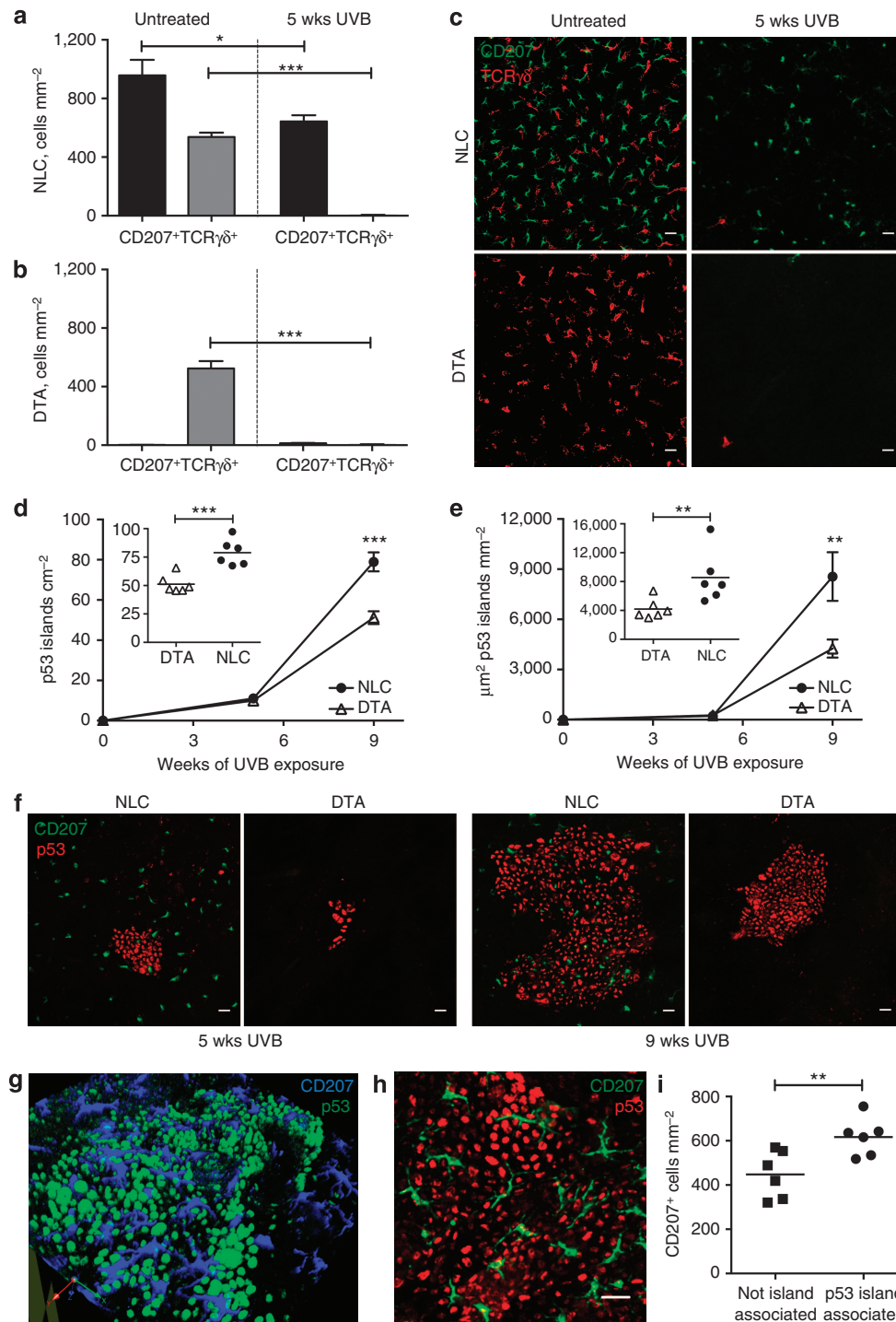


Figure 3. Langerhans cells (LCs) persist during chronic UVB exposure and facilitate p53 island formation. CD207⁺ LC and TCR γ δ ⁺ dendritic epidermal T cells (DETCs) were quantified in epidermal sheets prepared from untreated versus chronic UVB-treated (400 J m⁻², 3 \times /week, 5 weeks) (a) LC-intact normal littermate controls (NLC) and (b) LC-deficient hu-Langerin-DTA transgenic (DTA) hr/hr mice. (c) Representative images show CD207 (green) and TCR γ δ (red) staining. In both NLC and DTA mice, DETCs are nearly eliminated by chronic UVB treatment; however, LC in NLC mice are present at 66% of control levels following 5 weeks UVB exposure; *P < 0.05, ***P < 0.001, n = 6 mice/group. Mutant keratinocyte p53 (d) island density and (e) area were quantified in epidermal sheets prepared from n = 6 NLC and DTA hr/hr mice following 5 or 9 weeks of UVB exposure. Inset graphs show distribution at 9 weeks; each symbol represents one mouse, **P < 0.01, ***P < 0.001. (f and h) Representative images of p53 islands (red) and CD207⁺ LC (green), scale bar = 20 μ m, and (g) a 3D rendering of p53 (green) and LC (blue). (i) CD207⁺ LC density is increased in association with p53 islands; **P < 0.01. Quantitation is described in Supplementary Figure S3 online.

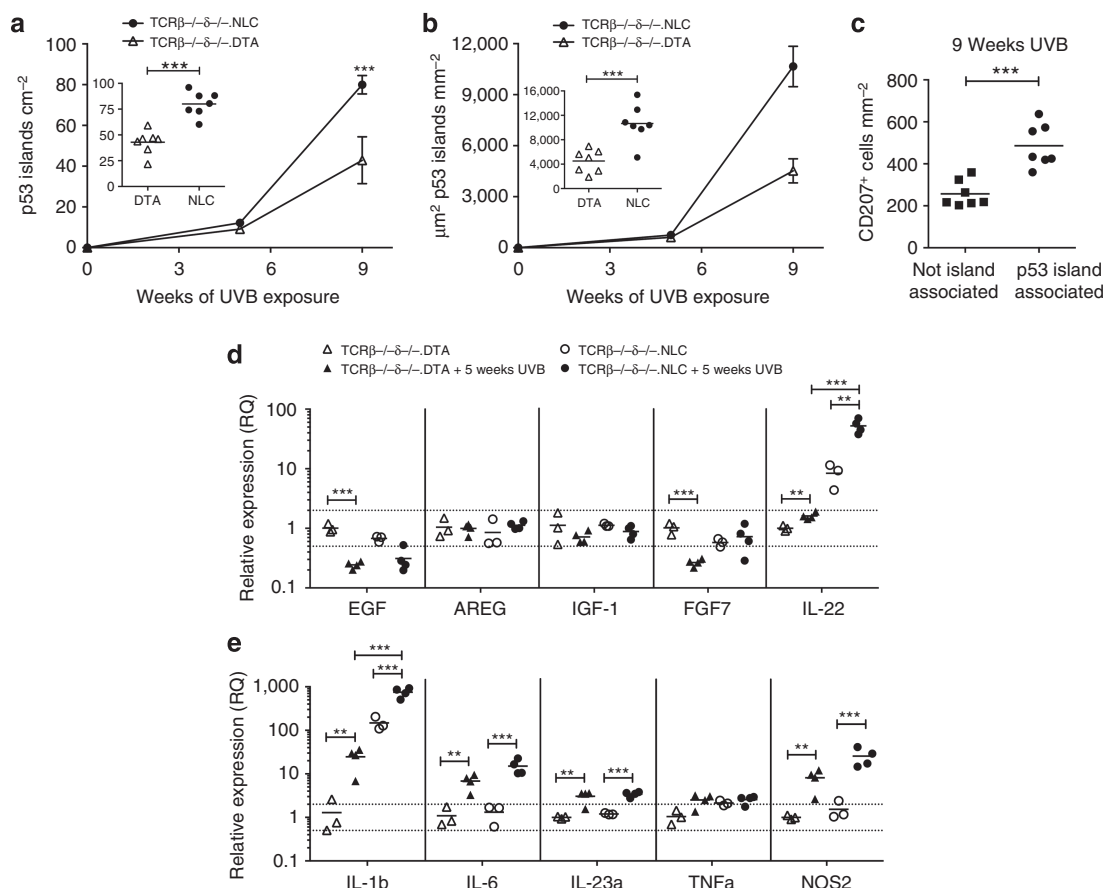


Figure 4. Langerhans cell (LC) facilitation of p53 island growth is T-cell independent. Mutant keratinocyte p53 (a) island density and (b) area were quantified in epidermal sheets prepared from $\text{TCR}\beta^{-/-}\delta^{-/-}\text{.NLC}$ (normal littermate controls) and $\text{TCR}\beta^{-/-}\delta^{-/-}\text{.DTA}$ (LC-deficient hu-Langerin-DTA transgenic) mice following 5 or 9 weeks of UVB exposure (400 J m^{-2} , $3\times/\text{week}$). Inset graphs show distribution at 9 weeks; each symbol represents one mouse. LC-intact $\text{TCR}\beta^{-/-}\delta^{-/-}\text{.NLC}$ mice have increased p53 island density and area compared with LC-deficient $\text{TCR}\beta^{-/-}\delta^{-/-}\text{.DTA}$ mice following 9 weeks UVB exposure; $***P<0.001$. (c) CD207^{+} LC density is increased in association with p53 islands. (d and e) Epidermal cells prepared from untreated versus 5 week chronic UVB-treated $\text{TCR}\beta^{-/-}\delta^{-/-}\text{.NLC}$ and $\text{TCR}\beta^{-/-}\delta^{-/-}\text{.DTA}$ mice were examined for changes in gene expression (relative to untreated $\text{TCR}\beta^{-/-}\delta^{-/-}\text{.DTA}$) by quantitative real time-PCR; each symbol represents one mouse, $**P<0.01$, $***P<0.001$, Holm-Sidak correction for multiple comparisons.

vs. untreated NLC, $P=0.0013$) and significantly higher in the presence of LCs (DTA+UVB vs. NLC+UVB, $P<0.0001$). In contrast, there were modest relative decreases or no discernible changes in the other assessed epithelial growth factors (Figure 4d). UVB-exposed LC-intact epidermis also displayed the highest levels of expression of IL-1 β and IL-6, and to a lesser extent IL-23a (Figure 4e), cytokines known to stimulate production of IL-22 by adaptive $\alpha\beta^{+}$ and $\gamma\delta^{+}$ Th22 cells as well as innate immune cells, e.g., NK and innate lymphoid cells (ILC) (Ahlfors *et al.*, 2014). NOS2, known to foster reactive oxygen species within the epidermis after UVB exposure (Chang *et al.*, 2003), was also the highest in UVB-exposed LC-intact epidermis. Furthermore, exposure of purified LCs to UVB *in vitro* resulted in increased expression of IL-1 β , IL-6, and IL-23a (Supplementary Figure S6 online), suggesting that at least a portion of the observed epidermal expression of these cytokines was attributable directly to LCs, as opposed to augmented production by KCs in the presence of LCs. Taken together, these data suggest that LC-intact

epidermis demonstrates enhanced KC and/or LC production of IL-1 β , IL-6, and (to a lesser extent) IL-23, which in turn supports local production of IL-22 by non-T (e.g., NK and/or ILC) cells.

IL-22-producing ILC3 populate chronically UVB-exposed skin

To determine the spectrum of immune cell populations present in T-cell-deficient LC-intact versus LC-deficient skin, suspensions prepared from $\text{TCR}\beta^{-/-}\delta^{-/-}\text{.NLC}$ and $\text{TCR}\beta^{-/-}\delta^{-/-}\text{.DTA}$ mice were analyzed by flow cytometry (Supplementary Figure S7 online). The only discernible difference in CD45^{+} MHC-II $^{+}$ cells from $\text{TCR}\beta^{-/-}\delta^{-/-}\text{.NLC}$ relative to $\text{TCR}\beta^{-/-}\delta^{-/-}\text{.DTA}$ skin was, as expected, the presence of LC populations (CD45^{+} MHC-II $^{+}$ CD11b^{+} CD207^{+} CD103^{-}) that included epidermal LC as well as apparent dermal “in transit” migratory LCs (Henri *et al.*, 2010). Although reduced in number following chronic UVB exposure, we found comparable levels between LC-intact and LC-deficient skin of the major dermal DC population

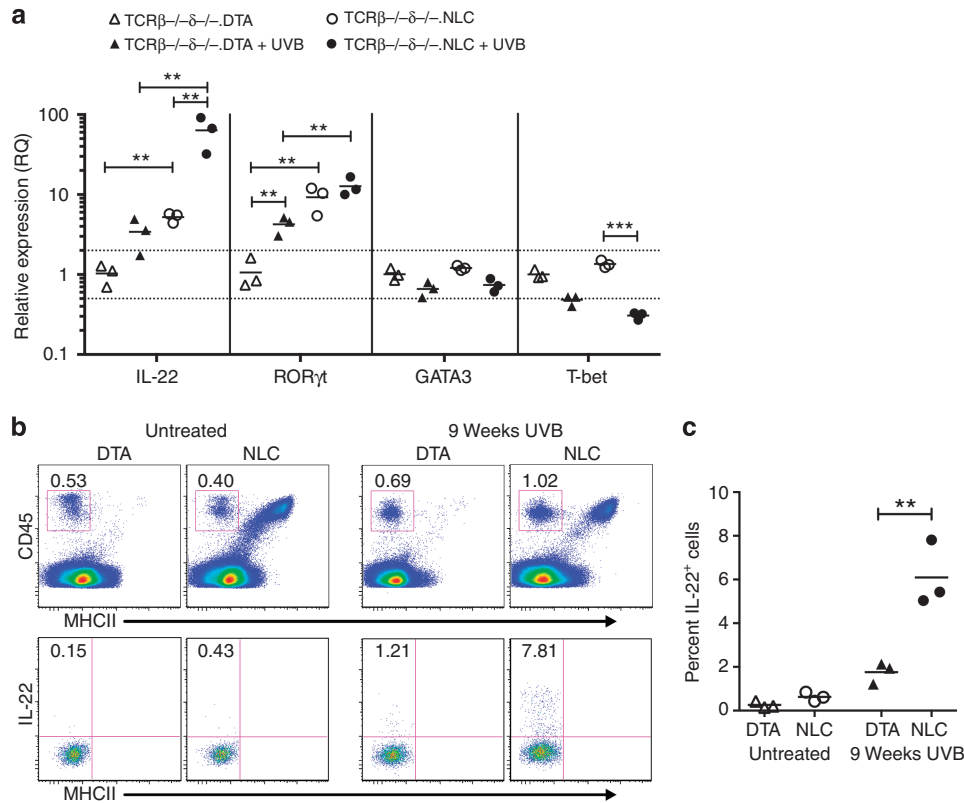


Figure 5. Epidermal innate lymphoid cells (ILC) produce IL-22 in response to chronic UVB exposure in the presence of Langerhans cells (LCs). (a) Epidermal ILC were purified from untreated and chronic UVB-treated (9 weeks, 400 J m⁻², 3 ×/week) TCRβ^{-/-}δ^{-/-}.NLC (normal littermate controls) and TCRβ^{-/-}δ^{-/-}.DTA (LC-deficient hu-Langerin-DTA transgenic) mice by flow cytometric sorting, and changes in gene expression (relative to untreated TCRβ^{-/-}δ^{-/-}.DTA) were assessed by quantitative real time-PCR; each symbol represents one mouse, ***P* < 0.01, ****P* < 0.001, Holm-Sidak correction for multiple comparisons. (b) Epidermal cells from individual untreated and 9-week chronic UVB-treated TCRβ^{-/-}δ^{-/-}.NLC and TCRβ^{-/-}δ^{-/-}.DTA mice were stimulated with phorbol 12-myristate 13-acetate+ionomycin and IL-22 production was assessed by flow cytometry. Top panels show CD45+ MHC-II⁻ gating, lower panels are gated on CD45+ MHC-II⁻ cells. Plots are representative of *n* = 3 mice/group. (c) Percentage of IL-22-producing CD45+ MHC-II⁻ epidermal cells; each symbol represents one mouse, ***P* < 0.01. MHC, major histocompatibility complex.

(CD45+ MHC-II+ CD11b+ CD207⁻ CD103⁻), the minor Langerin+ dermal DC population (CD45+ MHC-II+ CD11b⁻ CD207+ CD103+), and other dermal (CD45+ MHC-II+ CD11b⁻ CD103⁻) DCs. The epidermis of both TCRβ^{-/-}δ^{-/-}.NLC and TCRβ^{-/-}δ^{-/-}.DTA also harbors a population of CD45+ MHC-II⁻ CD11b⁻ IL-7R+ CD103+ cells that would be expected to contain ILC, and cells of this phenotype seemingly persist in UVB-treated skin (Supplementary Figure S8 online). Isolation and further analysis of both protein (flow cytometry) and mRNA (quantitative real time-PCR) expression (Figure 5) revealed the predominant differentiation phenotype to be consistent with IL-22-producing RORγt+ (Tbet⁻ GATA3⁻) ILC3 (reviewed in Artis and Spits, 2015). The proportion of CD45+ MHC-II⁻ epidermal ILC observed in TCRβ^{-/-}δ^{-/-} mice may be increased relative to that found in T-cell-intact mice as a compensatory mechanism similar to that previously reported for various immune cell populations in genetically modified mouse models, including cutaneous ILC (Roediger et al., 2013). Nonetheless, these ILC persist in chronically UVB-exposed epidermis, unlike DETCs, and the expression of IL-22 by these cells was substantially higher in

LC-intact epidermis after chronic UVB exposure (Figure 5), consistent with their activation and differentiation being positively influenced by both the presence of LCs and epidermal exposure to UVB.

The implication of LCs herein as a major contributor to UVB-induced p53 mutant KC clonal expansion via the enhancement of local production of IL-22 by ILC3, independently of resident or infiltrating T cells, suggests that LC may also have a more general role in epidermal homeostasis, including supporting KC proliferation as part of the epidermal stress response. Consistent with this hypothesis, at 5 weeks of UVB-exposure (a time with minimal difference in p53 island number and size between TCRβ^{-/-}δ^{-/-}.NLC and TCRβ^{-/-}δ^{-/-}.DTA; Figure 3d and e), we were able to detect greater epidermal thickness in association with the presence of LCs (Figure 6a and b). Removal of the stratum corneum and superficial KCs by repetitive tapestripping (Kuo et al., 2013) resulted in a greater transepidermal waterloss in TCRβ^{-/-}δ^{-/-}.NLC versus TCRβ^{-/-}δ^{-/-}.DTA epidermis (Figure 6c). More aggressive disruption of the epidermis by repetitive razor abrasion resulted in an even greater transepidermal waterloss in LC-intact epidermis that showed

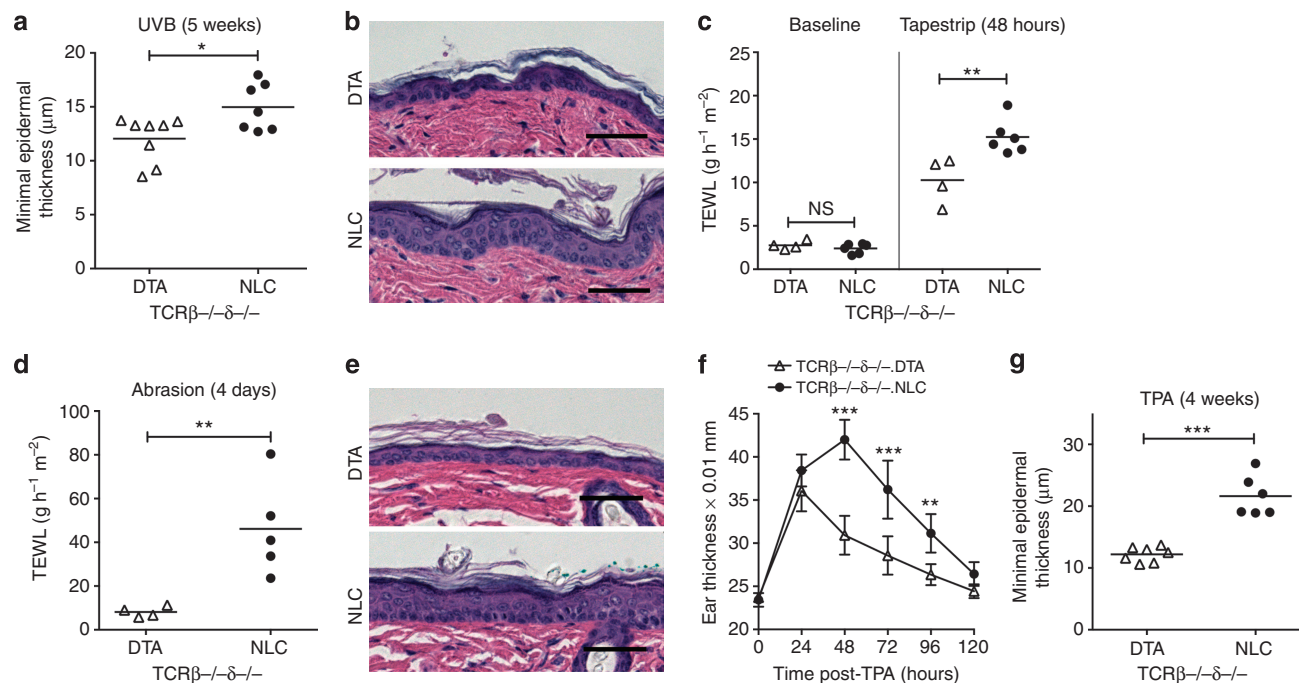


Figure 6. Langerhans cells (LCs) contribute to the epidermal stress response in a T-cell-independent manner. (a) Epidermal hypertrophy is greater in LC-intact $\text{TCR}\beta^{-/-}\delta^{-/-}$.NLC (normal littermate controls) than in LC-deficient $\text{TCR}\beta^{-/-}\delta^{-/-}$.DTA (LC-deficient hu-Langerin-DTA transgenic) mice following chronic UVB exposure (400 J m^{-2} , $3\times/\text{week}$, 5 weeks) as evaluated by measuring the minimal epidermal thickness. (b) Representative images of a. Transepidermal waterloss (TEWL) is equivalent at baseline but increased in LC-intact mice 48 hours after (c) tapestripping as well as 4 days after epidermal abrasion by (d) repetitive razor shaving. (e) Representative images of d. (f) Ear thickness following a single 12-O-tetradecanoylphorbol-13-acetate (TPA) application and (g) minimal epidermal thickness following twice weekly TPA for 4 weeks are greater in the presence of LCs. Each symbol represents one mouse in a, c, d, and g; $n=7$ NLC and 7 DTA in f. NS, not significant.

histological evidence of epidermal hyperplasia and hyperkeratosis (Figure 6d and e) and augmented expression of IL-22, IL-1 β , and IL-23 (Supplementary Figure S9 online). Furthermore, a single application of 12-O-tetradecanoylphorbol-13-acetate (TPA) provoked a greater ear swelling response in LC-intact skin (Figure 6f), while chronic TPA application ultimately showed enhanced epidermal thickening in association with the presence of LC (Figure 6g). These data are all consistent with LC serving as fundamental contributors to the epidermal stress response via stimulation of KC proliferation and dedifferentiation, independently of the presence of $\alpha\beta$ and $\gamma\delta$ T cells and regardless of the mode of epidermal damage (e.g., UV radiation, physical disruption, chemical irritant).

DISCUSSION

Immune cells resident within epithelial tissue have key roles in microbial defense and barrier homeostasis, and the activities of such cells may arrest or enhance carcinogenesis (Strid *et al.*, 2008; Yu *et al.*, 2014). The demonstration herein of a major role for LCs in UVB-induced skin carcinogenesis, as well as in the response to epidermal perturbation, further elucidates LCs as fundamental regulators of epidermal homeostasis. The pro-carcinogenic effect of LCs during UVB exposure is counter to the notion of LCs as key players in tumor immunosurveillance. Moreover, the demonstration that the association of LCs with p53 mutant KC clonal expansion is

completely independent of the presence of $\alpha\beta$ and $\gamma\delta$ T cells favors a mechanism in which LCs are directly affecting mutant KCs and/or stimulating non-T (NK and/or ILC) immune cells to induce an intraepidermal environment conducive to mutant KC survival and growth.

During chronic UVB exposure, the LC network remained largely intact (Figure 3). Whether the observed LC numbers were reflective more of a relative resistance to apoptosis of the initial resident population of LCs derived from fetal precursors, or from repopulating sources such as peripheral blood monocytes, is unclear. Nonetheless, Ki-67 staining reveals little evidence of active proliferation of LCs, in contrast to the clonally expanding mutant KCs (Supplementary Figure S2 online). The intimate association of LCs with the clonally expanding KC islands suggests the possibility that LCs detect and respond to dysregulated KCs or that the mutated KCs produce chemoattractant and/or survival factors for the LCs. Further investigation will be necessary to determine the relative contribution of LC enhancement of p53 mutant KC clonal expansion by direct (e.g., by local production of growth and/survival factors) versus indirect (e.g., by stimulation of other cells that produce growth and/or survival factors) influences and whether the LCs within expanding islands are functionally distinct from LCs not found in association with mutant KCs.

Our expression analysis of LC-intact and LC-deficient epidermal preparations, prior to and after chronic UVB

exposure, has provided insight into the nature of LC promotion of clonal expansion. Epidermal relative expression of IL-1 β , IL-6, and IL-23 were each observed to increase with UVB exposure in LC-deficient (TCR β –/– δ –/–.DTA) skin, consistent with known production of these cytokines by stressed KCs. In the presence of LCs (in TCR β –/– δ –/–.NLC), UVB-induced expression was significantly enhanced for IL-1 β and IL-6. Moreover, the substantial increase in the expression of IL-1 β in naive LC-intact versus LC-deficient epidermis (i.e., prior to UVB exposure) suggest that LCs may also have a role in homeostatic regulation of the epidermis. The augmented IL-22 expression observed in LC-intact skin chronically exposed to UVB is entirely consistent with increases in IL-1 β , IL-6, and IL-23—all known stimulators of IL-22 production.

Phenotypic analysis revealed that the augmented IL-22 production observed in association with the presence of LC and chronic UVB exposure may be attributable to ROR γ t+ ILC3 (reviewed in Artis and Spits, 2015). Thus UVB-exposed LC-intact epidermis supports an environment for the augmented expression by ILC3 of IL-22, a cytokine noteworthy for its stimulation of KC proliferation and de-differentiation, skin wound healing, and well-established association with epithelial carcinogenesis (reviewed in Lim and Savan, 2014). The receptor for IL-22 is primarily expressed by epithelial cells, including KCs, as a heterodimer (IL-22R1 and IL-10R2) that stimulates Stat3 activation, and a pro-carcinogenic role for IL-22 has been shown in models of colonic, lung, and hepatocellular carcinoma. Moreover, IL-22-producing ILCs were shown to be the principal drivers of dysplasia in a model of inflammatory bowel disease-associated colorectal cancer (Kirchberger et al., 2013).

The augmented local expression of IL-1 β , IL-23, and IL-22 following razor abrasion in the presence of LCs (Supplementary Figure S9 online) is also consistent with our observed responses to epidermal perturbation in (T-cell-deficient) LC-intact skin: increased epidermal hypertrophy, compromised epidermal barrier function, and augmented irritant response (Figure 6). Recombinant IL-22 can promote the *in vitro* survival and proliferation of KCs after mechanical disruption (Eyerich et al., 2009) and epidermal hypertrophy and dedifferentiation in reconstituted human epidermis (Rabeony et al., 2014). As LC numbers are largely maintained in human actinic keratoses (Shevchuk et al., 2014) and epidermal LC levels in organ transplant recipients are equivalent to controls (Sandvik et al., 2014), it is logical to investigate whether LCs are contributing to human SCC development. Clearly, further studies are necessary to more fully elucidate the relationship of LCs, ILC3, and IL-22 to epidermal homeostasis and UVB-induced cutaneous carcinogenesis.

MATERIALS AND METHODS

Animals and housing

FVB/N, DTA, NLC, TCR β –/–TCR δ –/– (TCR β –/– δ –/–.NLC) and TCR β –/–TCR δ –/–LC-deficient (TCR β –/– δ –/–.DTA) mice were previously described (Modi et al., 2012). Hairless mice (hr/hr, FVB/N background) were generously provided by Dr Donna Kusewitt

(The University of Texas MD Anderson Cancer Center, Houston, TX). All *in vivo* studies were approved by the Yale Animal Care and Use Committee.

UVB exposure

At age 7 weeks, hair was removed from the dorsal skin of female TCR β –/– δ –/–.NLC and TCR β –/– δ –/–.DTA mice by clipping plus depilatory cream; hr/hr mice were untreated. UVB exposures began at age 8 weeks using a bank of four FS20T12 broadband-UVB bulbs (National Biological, Corp., Twinsburg, OH) with emitted light filtered (Kodacel TA422, Eastman Kodak, Rochester, NY) to remove wavelengths <290 nm. Exposure was monitored using a calibrated meter and probe (Intensity Meter 200, G&R Labs, Santa Clara, CA). Chronic exposure consisted of 400 J m^{–2} 3 \times /weekly.

Tumor assessment

Tumors were measured, counted (when ≥ 1 mm²), and scored weekly as clinically apparent papillomas or carcinomas by a blinded observer as previously described (Girardi et al., 2003). Tumor volume was calculated as: $4/3\pi r^3$ where $r = (L \times W)/2$.

Immunofluorescence and confocal microscopy

Epidermal sheets were prepared and stained as previously described (Lewis et al., 2014) with anti-CD207 (RMUL2, eBioscience, San Diego, CA), anti-TCR $\gamma\delta$ (GL3, Becton Dickinson, Franklin Lakes, NJ), and anti-p53 (NCL-p53-CM5p, Leica Biosystems, Buffalo Grove, IL) followed by fluorescent species-specific secondaries (Jackson ImmunoResearch, West Grove, PA). Z-stacked images (20/mouse) were collected (Zeiss 510Meta confocal, Carl Zeiss Microscopy, Thornwood, NY) in a set pattern and Volocity 6.2 (Perkin Elmer, Waltham, MA) used to quantitate LCs and DETCs. CPD staining and quantification is described in Supplementary Figure S1 online and p53 island quantification in Supplementary Figure S3 online.

Epidermal cell suspensions and flow cytometry

Epidermal cell suspensions were prepared as described (Strid et al., 2008). For intracellular cytokine detection, cells were stimulated for 18 hours with 50 ng ml^{–1} phorbol 12-myristate 13-acetate plus 1 μ g ml^{–1} ionomycin. Monensin (2 μ M) was added for the final 6 hours plus Brefeldin A (10 μ g ml^{–1}) for the final 2 hours. Samples were blocked (2.4G2, BD Biosciences, San Jose, CA) and stained with antibodies to CD45 (30-F11, Biolegend, San Diego, CA), MHC-II (M5/114.15.2, eBioscience), IL-22 (Poly5164, Biolegend), or isotype controls, plus viability dye EMA. BD Biosciences CytoFix/CytoPerm Kit was used for fixation and permeabilization. Data were collected on Stratigigm S1000EX (Stratigigm, San Jose, CA) and analyzed with FlowJo (LLC, Ashland, OR). Cell sorting, to obtain CD45+ MHC-II– epidermal ILC, was performed on MoFlo (Beckman Coulter, Brea, CA).

Gene expression analysis

RNA was isolated (RNeasy, Qiagen, Valencia, CA) and transcribed (High-Capacity cDNA Reverse Transcription Kit, ABI, Carlsbad, CA). Quantitative real time-PCR (ABI 7500, SDS 2.0 software) was performed using Taqman assays and Taqman Gene Expression Mastermix (ABI). Ct values were normalized to β -actin, and expression differences relative to untreated DTA were calculated using $RQ = 2^{-\Delta\Delta Ct}$.

Epidermal stress response assays

Transepidermal waterloss was measured using the Tewameter TM300 (probe 06030433, Courage & Khazaka, Cologne, Germany). Tape-stripping consisted of three repetitions of adhesive tape application (Scotch Magic tape, 3M, St Paul, MN) performed 1 week following hair removal. Epidermal abrasion was induced by twice repeated shaving of ventral skin (Personna American Safety Razor, Verona, VA). Ear thickness following a single application of TPA (Sigma, St. Louis, MO, 0.5 nmoles) was measured using an engineer's micrometer (Mitutoyo 7301, Aurora, IL). Epidermal hypertrophy was induced by TPA (20 nmoles) application 2 x/week for 4 weeks. Histological examination and measurement of minimal epidermal thickness was performed as previously described (Lewis et al., 2014).

Statistical analysis

Statistical significance of differences in tumor number and volume (Figure 1) and ear thickness (Figure 6f) over time were assessed using repeated-measures analysis of variance with Sidak's correction for multiple comparisons. Differences in relative gene expression were assessed using Student's *t*-test for unpaired data with Holm-Sidak correction for multiple comparisons and establishment of significance. Other experimental groups were compared using one-tailed Student's *t*-test for unpaired data with significance established at *P* < 0.05. All statistical analyses were performed with the GraphPad Prism 6.0 software (GraphPad Software, Inc., La Jolla, CA).

CONFLICT OF INTEREST

The authors state no conflict of interest.

ACKNOWLEDGMENTS

Funding for this work was provided by the NIH grant R01CA102703 (to MG) and the Novartis Foundation for Medical-Biological Research (to CB). We thank A Hayday (CRUK) for insightful discussion, D Brash (Yale) for protocol advice, and D Kusewitt (MD Anderson) for providing FVB.hr/hr mice.

SUPPLEMENTARY MATERIAL

Supplementary material is linked to the online version of the paper at <http://www.nature.com/jid>

REFERENCES

- Aberer W, Romani N, Elbe A et al. (1986) Effects of physicochemical agents on murine epidermal Langerhans cells and Thy-1-positive dendritic epidermal cells. *J Immunol* 136:1210–6
- Ahlfors H, Morrison PJ, Duarte JH et al. (2014) IL-22 fate reporter reveals origin and control of IL-22 production in homeostasis and infection. *J Immunol* 193:4602–13
- Artis D, Spits H (2015) The biology of innate lymphoid cells. *Nature* 517: 293–301
- Bobr A, Igyarto BZ, Haley KM et al. (2012) Autocrine/paracrine TGF- β 1 inhibits Langerhans cell migration. *Proc Natl Acad Sci USA* 109:10492–7
- Briso EM, Guinea-Viniegra J, Bakiri L et al. (2013) Inflammation-mediated skin tumorigenesis induced by epidermal c-Fos. *Genes Dev* 27:1959–73
- Chan KS, Carbajal S, Kiguchi K et al. (2004) Epidermal growth factor receptor-mediated activation of Stat3 during multistage skin carcinogenesis. *Cancer Res* 64:2382–9
- Chang HR, Tsao DA, Wang SR et al. (2003) Expression of nitric oxide synthases in keratinocytes after UVB irradiation. *Arch Dermatol Res* 295:293–6
- Chikama T, Liu CY, Meij JT et al. (2008) Excess FGF-7 in corneal epithelium causes corneal intraepithelial neoplasia in young mice and epithelium hyperplasia in adult mice. *Am J Pathol* 172:638–49
- Daya-Grosjean L, Robert C, Drougard C et al. (1993) High mutation frequency in ras genes of skin tumors isolated from DNA repair deficient xeroderma pigmentosum patients. *Cancer Res* 53:1625–9
- DiGiovanni J, Bol DK, Wilker E et al. (2000) Constitutive expression of insulin-like growth factor-1 in epidermal basal cells of transgenic mice leads to spontaneous tumor promotion. *Cancer Res* 60:1561–70
- Durinck S, Ho C, Wang NJ et al. (2011) Temporal dissection of tumorigenesis in primary cancers. *Cancer Discov* 1:137–43
- Epstein JH (1983) Photocarcinogenesis, skin cancer, and aging. *J Am Acad Dermatol* 9:487–502
- Eyerich S, Eyerich K, Pennino D et al. (2009) Th22 cells represent a distinct human T cell subset involved in epidermal immunity and remodeling. *J Clin Invest* 119:3573–85
- Fukunaga A, Khaskhely NM, Ma Y et al. (2010) Langerhans cells serve as immunoregulatory cells by activating NKT cells. *J Immunol* 185:4633–40
- Girardi M, Oppenheim DE, Steele CR et al. (2001) Regulation of cutaneous malignancy by gammadelta T cells. *Science* 294:605–9
- Girardi M, Glusac E, Filler RB et al. (2003) The distinct contributions of murine T cell receptor (TCR)gammadelta+ and TCRalphabeta+ T cells to different stages of chemically induced skin cancer. *J Exp Med* 198: 747–55
- Henri S, Poulin L, Tamoutounour S et al. (2010) CD207+ CD103+ dermal dendritic cells cross-present keratinocyte-derived antigens irrespective of the presence of Langerhans cells. *J Exp Med* 207:189–206
- Ho KK, Halliday GM, Barnetson RS et al. (1991) Topical and oral retinoids protect Langerhans' cells and epidermal Thy-1+ dendritic cells from being depleted by ultraviolet radiation. *Immunology* 74:425–31
- Jameson J, Ugarte K, Chen N et al. (2002) A role for skin $\gamma\delta$ T cells in wound repair. *Science* 296:747–9
- Kaplan DH, Jenison MC, Saeland S et al. (2005) Epidermal langerhans cell-deficient mice develop enhanced contact hypersensitivity. *Immunity* 23: 611–20
- Kirchberger S, Royston DJ, Boulard O et al. (2013) Innate lymphoid cells sustain colon cancer through production of interleukin-22 in a mouse model. *J Exp Med* 210:917–31
- Kripke ML (1984) Immunological unresponsiveness induced by ultraviolet radiation. *Immunol Rev* 80:87–102
- Kubo A, Nagao K, Yokouchi M et al. (2009) External antigen uptake by Langerhans cells with reorganization of epidermal tight junction barriers. *J Exp Med* 206:2937–46
- Kuo IH, Carpenter-Mendini A, Yoshida T et al. (2013) Activation of epidermal toll-like receptor 2 enhances tight junction function: implications for atopic dermatitis and skin barrier repair. *J Invest Dermatol* 133: 988–98
- Kwong BY, Roberts SJ, Silberzahn T et al. (2010) Molecular analysis of tumor-promoting CD8+ T cells in two-stage cutaneous chemical carcinogenesis. *J Invest Dermatol* 130:1726–36
- Lewis JM, Bürgler CD, Fraser JA et al. (2014) Mechanisms of chemical cooperative carcinogenesis by epidermal langerhans cells. *J Invest Dermatol* 135:1405–14
- Lim C, Savan R (2014) The role of the IL-22/IL-22R1 axis in cancer. *Cytokine Growth Factor Rev* 25:257–71
- MacLeod AS, Rudolph R, Corriden R et al. (2014) Skin-resident T cells sense ultraviolet radiation-induced injury and contribute to DNA repair. *J Immunol* 192:5695–702
- Merad M, Manz MG, Karsunky H et al. (2002) Langerhans cells renew in the skin throughout life under steady-state conditions. *Nat Immunol* 3: 1135–41
- Modi BG, Neustadter J, Binda E et al. (2012) Langerhans cells facilitate epithelial DNA damage and squamous cell carcinoma. *Science* 335:104–8
- Nishibu A, Ward BR, Jester JV et al. (2006) Behavioral responses of epidermal Langerhans cells in situ to local pathological stimuli. *J Invest Dermatol* 126: 787–96
- Rabeony H, Petit-Paris I, Garnier J et al. (2014) Inhibition of keratinocyte differentiation by the synergistic effect of IL-17A, IL-22, IL-1 α , TNF α and oncostatin M. *PLoS One* 9:e101937

- Rittié L, Varani J, Kang S *et al.* (2006) Retinoid-induced epidermal hyperplasia is mediated by epidermal growth factor receptor activation via specific induction of its ligands heparin-binding EGF and amphiregulin in human skin in vivo. *J Invest Dermatol* 126:732–9
- Roediger B, Kyle R, Yip K *et al.* (2013) Cutaneous immunosurveillance and regulation of inflammation by group 2 innate lymphoid cells. *Nat Immunol* 14:564–73
- Sandvik LF, Skarstein K, Sviland L *et al.* (2014) CD11c(+) dendritic cells rather than Langerhans cells are reduced in normal skin of immunosuppressed renal transplant recipients. *Acta Derm Venereol* 4:173–8
- Seneschal J, Clark RA, Gehad A *et al.* (2012) Human epidermal Langerhans cells maintain immune homeostasis in skin by activating skin resident regulatory T cells. *Immunity* 36:873–84
- Séré K, Baek JH, Ober-Blöbaum J *et al.* (2012) Two distinct types of Langerhans cells populate the skin during steady state and inflammation. *Immunity* 37: 905–16
- Shreedhar VK, Pride MW, Sun Y *et al.* (1998) Origin and characteristics of ultraviolet-B radiation-induced suppressor T lymphocytes. *J Immunol* 161: 1327–35
- Shevchuk Z, Filip A, Shevchuk V *et al.* (2014) Number of Langerhans cells is decreased in premalignant keratosis and skin cancers. *Exp Oncol* 36: 34–7
- Strid J, Roberts SJ, Filler RB *et al.* (2008) Acute upregulation of an NKG2D ligand promotes rapid reorganization of a local immune compartment with pleiotropic effects on carcinogenesis. *Nat Immunol* 9:146–54
- Wakita D, Sumida K, Iwakura Y *et al.* (2010) Tumor-infiltrating IL-17-producing gammadelta T cells support the progression of tumor by promoting angiogenesis. *Eur J Immunol* 40:1927–37
- Wang L, Jameson SC, Hogquist KA (2009) Epidermal Langerhans cells are not required for UV-induced immunosuppression. *J Immunol* 183:5548–53
- Yu SH, Bordeaux JS, Baron ED (2014) The immune system and skin cancer. *Adv Exp Med Biol* 810:182–91
- Zhang W, Remenyik E, Zeltermann D *et al.* (2001) Escaping the stem cell compartment: sustained UVB exposure allows p53-mutant keratinocytes to colonize adjacent epidermal proliferating units without incurring additional mutations. *Proc Natl Acad Sci USA* 98:13948–53
- Ziegler A, Jonason AS, Leffell DJ *et al.* (1994) Sunburn and p53 in the onset of skin cancer. *Nature* 372:773–6